Panel Method for Aero-Propulsive Design Space Exploration

Africawala, Jalendu, Joksimović Aleksandar

Panel Method for Aero-Propulsive Design Space Exploration

Jalendu Africawala *, Aleksandar Joksimović †
ISAE-SUPAERO, Université de Toulouse, France

The paper presents development of a low-order preliminary design tool based on panel methods, dedicated to analysis of the aero-propulsive design space for civil aviation applications. The development is building upon previous preliminary endeavours done by the same team, based on the idea of generalisation of an existing approach found in the literature. To enable full liberty to the designers, the tool is structured around a two-dimensional representation of an aero-propulsive assembly which consists of an integrated wing aerofoil, a nacelle aerofoil and a propulsor in-between the two. To enable the capability to the designers to investigate any aero-propulsive concept of interest by applying the panel method to the described setup, designers can independently modify any major geometric parameter of the assembly, along with the propulsive power input and the free stream flow characteristics. The additional integral part of this geometric setup consists of an artefact necessary to take along to enable panel method/irrotational modelling for a powered flow - a propulsive jet emanating from the propulsor. The presented developments of the tool concern the full geometrical parametrisation and improvement of the numerical scheme for more robust iteration of the propulsive jet shape. The tool is verified to be capable of operating across a very large design space and the method performs well for flows around clean geometries. Preliminary validation for the aero-propulsive case is not conclusive, and further work needs to be done to resolve uncertainties concerning the various aspects of the simplified propulsive jet model.

I. Nomenclature

API	=	Application Programming Interface
BC	=	Boundary Condition
BLI	=	Boundary-Layer Ingestion
CFC	=	Computational Fluid Dynamics
c	=	Chord
c_{base}	=	Chord length of the base airfoil
$c_{nacelle}$	=	Chord length of the nacelle airfoil
C_p	=	Pressure coefficient
Cl	=	Lift coefficient
CPU	=	Central Processing Unit
$F_{z,jet}$	=	Vertical component of the jet thrust at the nozzle
$F_{z,pressure}$	=	Integrated vertical pressure force on the jet surfaces
$F_{z,pressure,RES}$	=	Integrated vertical pressure force on the trailing 5% of jet surfaces
H	=	Height/depth of the trailing jet
IC	=	Initial Conditions
$J(h)$	=	Cost function of the jet's depth
L_{dop}	=	Height/depth of the trailing jet
L_T	=	Length of the trailing jet
LE	=	Leading Edge
$\hat{n}$	=	Normal vector to the panel
n_i	=	Normal vector to panel i
r_{ij}	=	Radial distance between i and j panel
t_i	=	Tangential vector to panel i

*Graduate student, Department of Aerodynamics, Energetics and Propulsion.
†Associate Professor, Department of Aerodynamics, Energetics and Propulsion, corresponding author, aleksandar.joksimovic@isae-supaero.fr.

T	=	Jet thrust
V_∞	=	Free-stream velocity
V_x	=	Free-stream velocity in x-direction
V_y	=	Free-stream velocity in y-direction
V_N	=	Normal velocity
V_n	=	Normal velocity
x	=	X-coordinate
x_{inlet}	=	Fan's x-axis distance from the base airfioil leading edge
y	=	Y-coordinate
$y_{nacelle}$	=	Y-axis distance between the base airfoil leading edge and the nacelle
α	=	(aerodynamic model context) Angle of attack
α	=	(optimisation code context) Learning rate
β_i	=	Angle between panel's normal vector and the free-stream velocity
γ_i	=	Vortex elementary flow strength
δ_i	=	Angle between panel's normal vector and the x-axis
θ	=	Angle between trailing jet's camber line and x-axis
θ_1	=	Angle between freesteam angle of attack and jet trailing edge
θ_{ij}	=	Angular distance between i and j panel
λ_i	=	Source/sink elementary flow strength
τ	=	Angle between nacelle and the x-axis

II. Introduction

To date, civil aircraft design space is dominated by so-called "Tube and Wing" concepts, where a pre-set number of podded gas-turbine engines are mounted on the airframe generate the thrust. Although this design is sound, engine installation issues are becoming more prominent with ever-increasing turbofan engine size (i.e. the bypass ratio), which has historically been the way to respond to the demand for mission fuel reduction. However, system-level efficiency attainable that way seems to be saturating. [1] Hence, in light of increasingly tighter grip around the aeronautical sector for its high environmental footprint compared to the relative size of the industry [2], seeking more performant solutions is always of interest. Exploring novel aircraft morphologies is a critical factor in overcoming these issues. [1] Although they seem to have fallen out of favour in the mainstream industry following the post-Covid period, concepts relying on synergies between the airframe and the propulsion systems in principle remain interesting performance-, that is energy-wise. One example of such concept includes NASA's *N3-X*, which relies on turbo-electric distributed propulsion architecture with boundary layer ingestion on the suction surface of a blended-wing body [3]. Distribution of the generated thrust into an arbitrary number of big or small contributions (i.e. few big propulsors or many small propulsors) enabled by electrical transmission systems generate a theoretical abundance of architectural and/or configurational options which could all go under the same descriptive umbrella of "aero-propulsive concepts". Theoretical benefits of airframe and propulsion system synergies have been explored extensively in the literature. [4–6] A sample of the size and extent of the concept space based on the principle of boundary-layer ingestion (BLI), distributed propulsion, and wake filling with a proposal for a taxonomy of such concepts can be found e.g. in review presented by Bijewitz et al. [1] Another useful illustration is the design space presented by Wick et al. [7] in the framework of extensive 2D-CFD-based exploration of concept space based on strong aero-propulsive integration. (Fig.1)

Hendricks [8] presented a review of available approaches to model BLI in conceptual design, and the scope and variety thereof is more extensive than what has been common in the conventional conceptual design. This is a reflection of the inherent problem of venturing into the new design space whose theoretical scope grows combinatorially with different propulsion options (architectures and configurations thereof) as well as airfame geometrical configurations: among the vast population of possible concepts, how do we perform decision-making in conceptual design with a solid degree of confidence at low computational cost? While experiment and CFD software remain the primary methods for analysing such concepts, they demand extensive time and/or CPU resources. For the sake of the argument, if a certain CPU budget is assumed to be allocated in preliminary design, finding an optimal solution in a huge design space implies two extreme possibilities. On the one hand, one could consolidate all the available resources and time in order to precisely explore a very small number of possible solutions, which is what is done in detailed design, assuming that the preliminary design is successful. Inversely, one could *dilute* the precision and explore the broad design space extensively, which is the domain of preliminary design. The work presented in the current paper is motivated by the

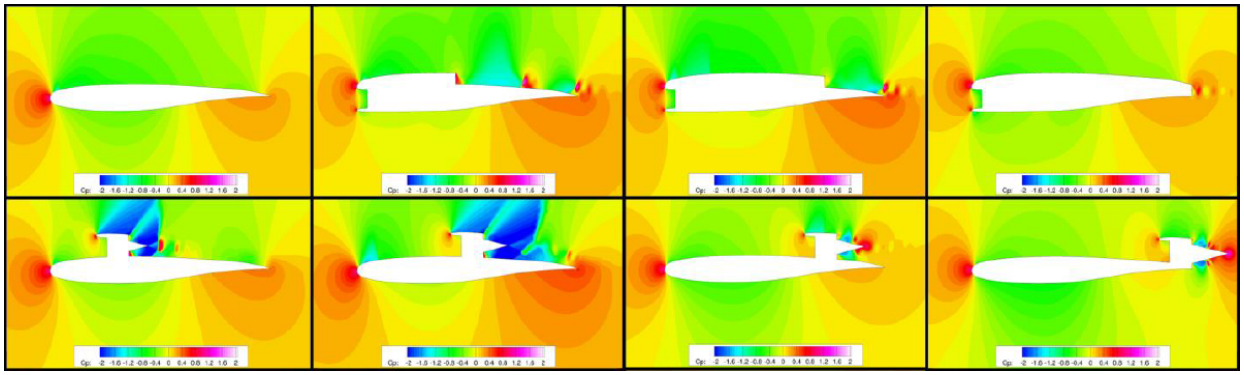

Fig. 1 Illustration of a much more extensive concept space in two dimensions, itself also just a small sample of what is conceivable by virtue of aero-propulsive integration; presented by Wick et al. [7]

latter scenario, aiming to develop a low-order tool to address a very broad range of varied aero-propulsive configurations at preliminary design level.

A similar initial version of a tool which could begin to give first-order responses to these questions was previously developed by the same team at ISAE-SUPAERO, as presented by Bommidala et al. [9]. The current paper focuses on following up on the previous work on developing an in-house low-fidelity tool for low-order aero-propulsive assembly analysis using the panel method approach. The methods explored for this tool were inspired by the works from the literature [10], which ventured to use the panel method approach to administer an elementary model of a specific aero-propulsive configuration. They aimed at predicting inviscid flow around a two-dimensional an aero-propulsive system consisting of an aerofoil with flaps, fans, distributed suction at the inlet, and a jet geometry from the trailing edge. The current paper presents further efforts in consolidation, development and verification thereof. The objectives of the paper are:

1) In line with the previous work [9], further development of a panel method tool capable of handling both conventional clean profiles and aero-propulsive configurations;
2) Expanding the tool's capabilities to cover a larger design space of the aero-propulsive architecture concepts than what was previously possible, i.e. solely a concept with the propulsor fixed on the suction surface trailing edge zone of the airframe;
3) The tool relies on including a propulsive jet model (cf. section III below); part of the presented work consists on implementing a gradient-based optimisation technique to improve the model convergence when employing it beyond the concept space originally considered by the previous authors;
4) Preliminary verification and validation of the new version of the tool by comparison with clean airfoil polars and pseudo-validation for aero-propulsive configurations by comparing with Euler CFD results for the same configurations.

III. Background for the Presented Work

Numerous studies of aero-propulsive synergies have been performed to evaluate potential advantages for vehicle-level energy- and/or fuel efficiency. As argued previously, up to date the sole available method that enables full concept flexibility remains numerical approach, i.e. CFD. With the current work being focused on exploring tools for the design space exploration, which operate at low computational cost, it was more relevant to search the literature for low-order methods.

Authors like Spence [11] and Albers & Potter [10] have developed potential flow methods to investigate such concepts over fifty years ago. In particular, Spence formulated a potential-flow based approach for a high-lift wing (jet-flap) system [11] that used vortex sheets to model the shape of the jet emanating from the airfoil, but its utilisation was limited to slender airfoils and evidently did not take into the account any flow suction as would be the case for an aero-propulsive concept. Albers & Potter [10] worked on developing a method to predict potential flow for a particular assembly consisting of a flapped airfoil and a propulsor mounted on the pressure side. (Fig.2(a)) The motivation for their development was to have a low-order model of the particular aero-propulsive configuration of interest, for purposes of short take-off and landing analysis. The authors assumed that the wing-propulsion system works in unison, treating it as

a single entity with suction zone at the fan inlet. To remain coherent with the principles of potential flow modelling, i.e. to account for the fact that the jet stream from the propulsion system has higher total pressure than the surrounding flow, the jet was "incorporated" into the model by extending the solid boundary of the aero-propulsive assembly to encompass the contour of the jet. Figure 2(b) shows the translation of the configuration into a panel-method computational setup, which enables calculation of the pressure distribution, flow fields, and in turn the lift coefficient for this configuration. The authors considered the wing, the nacelle, and the jet as having no mixing, so the normal velocity on these surfaces is zero. However, the inlet of the propulsor had a prescribed normal velocity. They described the jet using variables such as angle, penetration, and length, and assumed the jet angle was the same as the flap angle. They found that the lift coefficients and pressure distributions for the jet depend on the flap angle and jet penetration, and not the local shape of the jet.

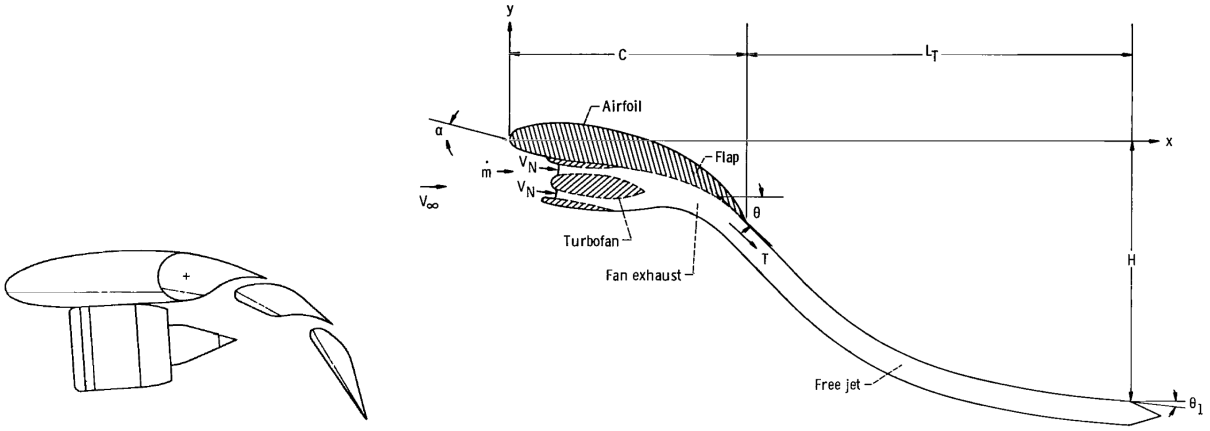

(a) Real-life blown wing configuration. **(b) Equivalent geometry for panel method, with the propulsive jet included.**

Fig. 2 Elementary two-dimensional schematic representation of an aero-propulsive assembly, for the particular configuration studied by Albers & Potter. [10]

Leaning on the work from Spence, Jois&Ansell [12] have undertaken a similar development based on potential flow modelling using infinitely thin jet flaps, but without resorting to explicit representation of a propulsor. Namely, their approach to low-order modelling of aero-propulsive configurations performance relies on jet vortex sheets representing the total pressure added to the flow, which models the necessary assembly-level information on pressure distribution and the resulting aerodynamic coefficient, but without capturing any detail about the propulsor itself: its position, added power and efficiency.

The work to which the current paper contributes is based on the premise of taking the approach proposed by Albers & Potter as a starting point, and parametrising it in such a way that a comprehensive design space could be recovered, akin to what Wick et al. [7] explored with two-dimensional CFD. To that end, development of a Python-based tool aiming to enable such capability was initiated at ISAE-SUPAERO [9]. The next chapter presents the relevant details thereof (Sec.IV.B) before the ongoing developments are elaborated.

IV. Aero-Propulsive Panel Method Development

This chapter provides an overview of the methodology employed for the tool, followed by a tool verification study. The development of the tool is done in three steps. Firstly, the coded panel method is verified for clean airfoil cases for manageable verification and preliminary validation. Then, a nacelle is added to create a proto-aero-propulsive case, to assess the tool behaviour for a geometry more complicated than a simple aerofoil. The final step consists of implementing the full setup of the two-dimensional aero-propulsive architecture as described in the previous chapter.

A. Summary of the Underlying Panel Method

The first step in modelling the aerodynamic behavior of aero-propulsive architectures along the lines of the chosen reference, namely using panel methods - is to formalise the potential, i.e. inviscid, irrotational, and incompressible

flow over impenetrable contours. Laplace's equation is used to model potential flows; it can be derived using the mathematical equations for inviscid and incompressible flow (e.g. see Katz&Plotkin [13]). For the panel method employed in this tool, the airfoil was discretised into n number of panels. For each panel, the respective geometrical properties of each panel were determined as illustrated in Fig.3. Discrete vortex and source/sink were used as the elementary solutions to model the flow over the airfoil. Hybrid elementary solutions (discrete source and vortex flows) allows improvement in flow resolution capabilities.

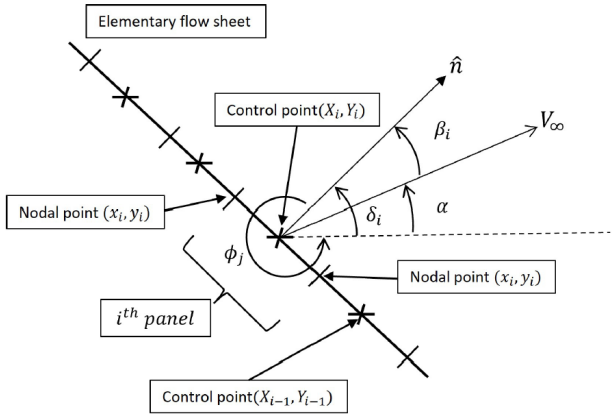

Fig. 3 Schematic representation of the geometric properties of a panel.

At the control point of the panels, defined to be at the centre of the panel, the influence of free-stream velocity and induced velocities at panel i due to panel j is solved in the vectorial direction normal to the panel. In order to assert the no-flux condition at each panel, eq.1 is imposed. Moreover, the Kutta condition is enforced for the flow to leave the trailing edge parallel on both sides, i.e. with velocity at the trailing edge equal both on the suction and the pressure surface. (eq.2)

$$V_{ind} \cdot \vec{n} + V_\infty \cdot \vec{n} = 0 \tag{1}$$

$$V_{t,1} + V_{t,N} = 0 \tag{2}$$

The influence of discrete source panel and discrete vortex panel distribution on a panel i due to a panel j in normal and tangential directions are given by eqs.3-6.

$$V_{n,i} = \sum_{j=1}^{N} \frac{\lambda_j}{2\pi} \cdot \int_j \frac{\delta}{\delta n_i} ln(r_{ij}) ds_j \tag{3}$$

$$V_{n,i} = \sum_{j=1}^{N} \frac{-\gamma}{2\pi} \int_j \frac{\delta \theta_{ij}}{\delta n_i} ds_j \tag{4}$$

$$V_{t,i} = \sum_{j=1}^{N} \frac{\lambda_j}{2\pi} \cdot \int_j \frac{\delta}{\delta t_i} ln(r_{ij}) ds_j \tag{5}$$

$$V_{t,i} = \sum_{j=1}^{N} \frac{-\gamma_j}{2\pi} \int_j \frac{\delta \theta_{ij}}{\delta t_i} ds_j \tag{6}$$

B. Baseline Panel Tool Adapted to Aero-Propulsive Applications

A brief overview of the baseline version of the tool developed by the previous authors [9] is provided before proceeding to elaborate on the latest developments. The schematic of the initial configuration is shown in Fig.4. The work was done on resolving the flow using panel method for a configuration that used $ms0313$ as the base airfoil and $NACA0012$ as nacelle airfoil. The tool could handle one aero-propulsive geometry where the nacelle was located on

the suction side of the base airfoil and their trailing edges were tangential to the jet emanation curves. They further trailed a jet geometry similarly to Albers & Potter [10]. The jet was defined using three parameters: jet angle θ which intended to imitate flow deflected by a flap, jet length L_t, and jet depth of penetration L_{dop}. The velocity calculations for the fan suction was done using basic *0D* thermodynamic models (see e.g. [14]) written in a coupled module; it thus enables using the fan power and efficiency as boundary condition for the design, in addition to the geometry and flight conditions boundaries conventionally used in clean airfoil analysis. Note that in this rudimentary version of the tool no boundary layer flow estimation is done, so no subsequent information thereof is carried over to the fan efficiency: i.e. in practice the fan is modelled the same as if it were a conventional clean-inflow fan. The previous authors further employed a preliminary jet shape iteration algorithm in order to define and converge the jet shape based on its adaptation to the free-stream flight conditions.

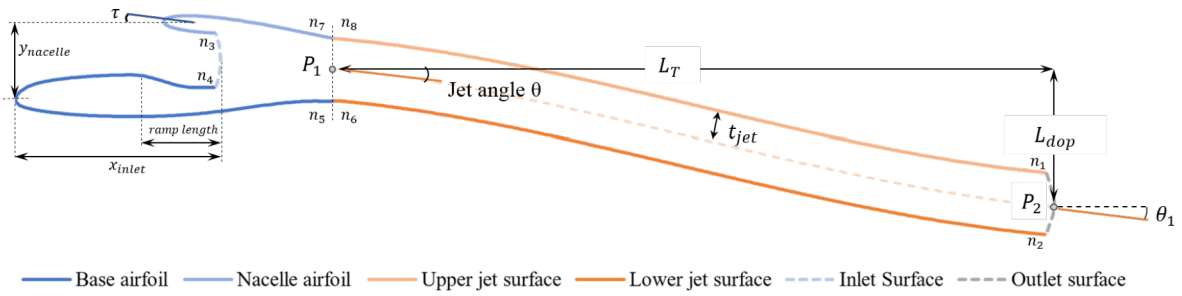

Fig. 4 Initial aero-propulsive configuration description and the associated parametrisation. [9]

Moreover, the initially developed panel tool considered the base airfoil, the nacelle, and the jet geometry as impenetrable; namely, the boundary condition imposed on these surfaces was no velocity flux in the direction normal to the respective surfaces. Furthermore, the fan inlet was imposed with a finite normal velocity calculated using the *0D* thermodynamics model. The potential flow solver employing panel method approach iterated to find a flow solution for the geometry from which the pressure distribution over the surfaces could be calculated. Using the pressure distribution on the jet surfaces the shape would be modified and with new flow solution being calculated. This process would be iterated onto until a jet shape convergence. The additional details regarding this version of the algorithm can be found in reference [9].

Important drawbacks of the previous tool, which motivated the work presented in this paper, were the following:

1) The tool could analyse only one aero-propulsive configuration, exactly as the one illustrated in Fig.4, with its use restricted only to modifying the configuration by nacelle relocation and chord modification of the two airfoils;
2) The jet shape modification module was not robust enough to converge for all configurations, for example for a wider range of jet angles.

C. Further Development of the Tool

The expansion of tool's capabilities is directed towards capability to resolve the flow for an extensive variety of configurations combinatorially enabled by the available design variables: geometrical details of the aero-propulsive assembly and the propulsive power setting (power and efficiency of the propulsor), thus capturing the overall external aerodynamic performance of the assembly as a function of any of the said design variables. While efforts were made to provide freedom to relocate the nacelle anywhere relative to the main airfoil, it demanded a more robust propulsive jet shape determination algorithm. Therefore, the former jet shape determination module was upgraded with a more sophisticated optimisation algorithm for facilitating convergence. Gradient-based optimisation algorithm not only allowed more robust jet shape convergence, but it also permitted changing the jet angle, which allows to approximate effects of deploying high-lift devices on the overall aerodynamic performance of the assembly.

1. Extension of the Aero-Propulsive Geometry Characterisation

The current tool allows the designers to navigate the geometric design space, that is to independently modify the base chord, the nacelle chord, and the nacelle position anywhere between the leading and the trailing edge of the base airfoil, either on the suction or the pressure side. In addition, the tool allows rescaling of the nacelle and changing its

angle of attack relative to the base airfoil. While these configurations consist of embedding propulsor within the lifting surfaces, a ramp can also be incorporated to represent a typical propulsor embedding. Figure 5 presents a sample of the possible configurations that can be designed using the tool.

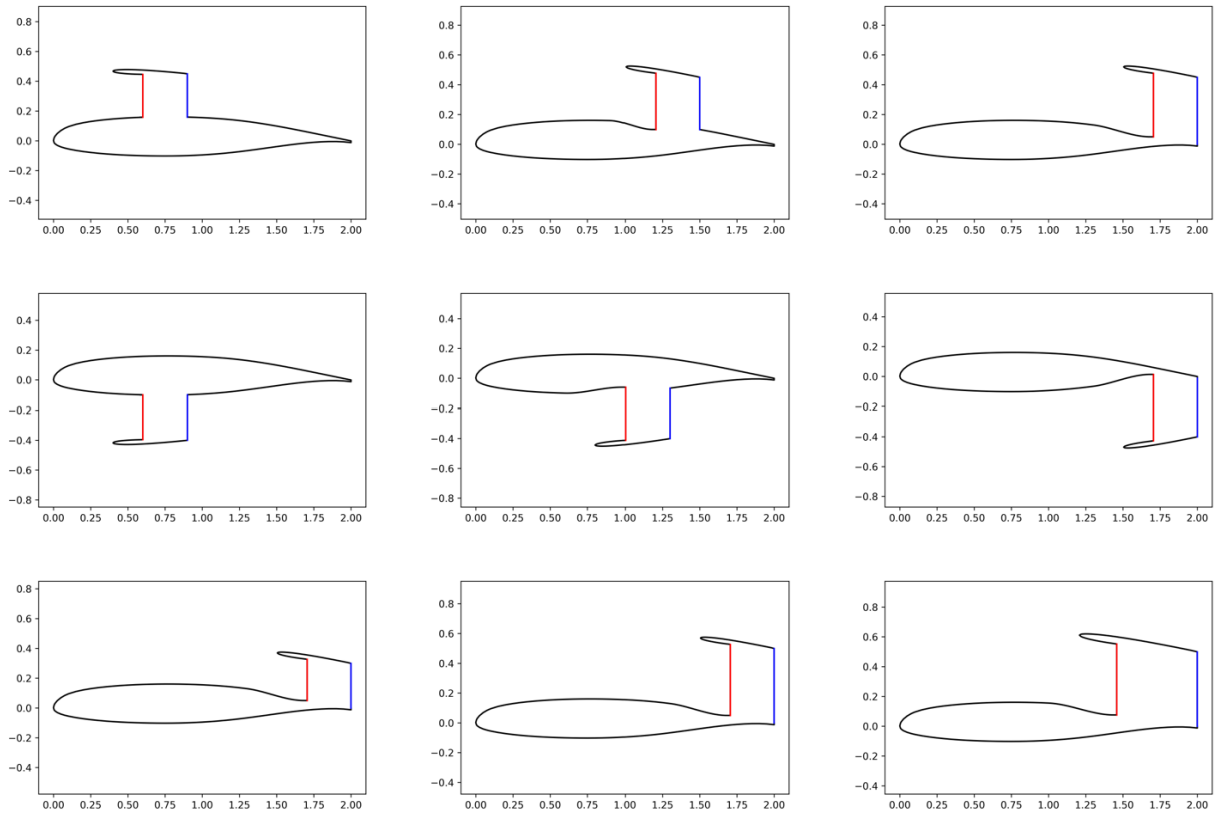

Fig. 5 Sample visuals of the tool's capabilities to model different two-dimensional aero-propulsive geometries.

Although the tool gives liberty to relocate the nacelle to explore influence of different configurations on aerodynamic performance, there remains a technical gap in representing the jet for all possible configurations (especially when the nacelle is upstream to the trailing edge of the base airfoil). While our knowledge is restricted to trailing a jet shape only after the trailing edge (as learned from Albers & Potter [10] and Spence [11]), it was essential to find a solution to bridge this gap and suggest how to model jet shape between propulsor nozzle and trailing edge of the base airfoil when the nacelle is upstream to the trailing edge of the base airfoil. An upstream prolongation of the jet shape was implemented by geometrically modelling the segment as an offset of the base airfoil curve portion blown by the jet. This curve is inserted between the propulsor nozzle and the jet emanation point at the trailing edge. The basic assumptions considered in favour of this choice were:

1) The nozzle is shaped in a manner that allows perfect expansion of the jet at the nozzle exit,
2) This portion of the jet predominantly follows the airfoil shape.

Concerning the jet speed evolution over the blown part of the airfoil, it was decided to transmit the jet exhaust information from station 9 (nozzle ejection point) to the trailing edge without any variation, so a more representative model of that zone needs to be included at a later stage if we are to have any confidence in the assemblies with forward-placed propulsors. Subsequently, the paneling and solver routines were preserved from the previous version; however, efforts were made to make the jet shape determination algorithm more robust with the help of optimisation techniques.

2. Gradient Descent Optimisation for Jet Shape Determination

With the expansion of tool capabilities to model varied aero-prop architectures and employ different jet exhaust angles (θ), it becomes essential to have a robust algorithm to converge the jet shape abiding with the following criteria:

1) Vertical thrust of the jet at nozzle ($F_{z,jet}$) be equivalent to vertical integrated pressure force from the jet surfaces ($F_{z,jetpressure}$).

$$F_{z,jet} = F_{z,jetpressure} \tag{7}$$

2) The vertical integrated pressure force on the last 5% ($F_{z,jetpressure,RES}$) of the jet length is negligible. It was decided to fix the length of the jet to be 4 times that of the chord of the base airfoil to have negligible integrated pressure of the last 5% of the jet. The hypothesis is based on the Albers&Potter's findings [10].

Parametric studies of varied jet depth illustrated the proportionality between the vertical component of the integrated pressure force and the jet depth. Moreover, this is a single-variable problem where the relationship between the jet depth and the integrated vertical pressure force cannot be determined analytically. For the mentioned optimisation problem, population-based optimising algorithms (e.g. Genetic Algorithm, Particle Swarm Optimisation, etc.) are often employed. However, these population-based optimisers demand a data pool, out of which the fittest are chosen. With the combinatorial possibilities for aero-prop configurations, it poses an eminent challenge to generate such data pool. Therefore, gradient-based algorithms were considered fit for this problem, with their robustness and implementation simplicity. The methods to implement gradient descent algorithm to optimise the jet shape are as elaborated in the following:

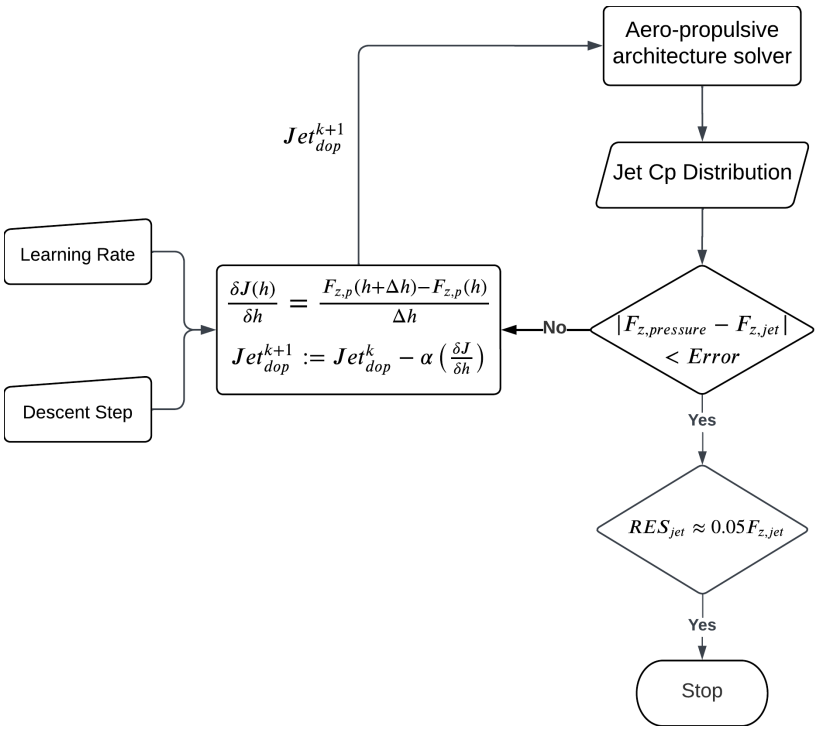

Fig. 6 Gradient descent optimisation algorithm for the jet shape determination.

1) Define a cost function to be minimised that relates the jet's vertical momentum force to jet's integrated lift;
2) Calculate the partial derivative of the function with respect to the jet's depth. This derivative is used for updating the value of integrated vertical pressure force in the gradient descent algorithm;
3) Initialise the jet with a chosen depth and length;
4) Calculate the value of the function for the current jet depth value;
5) Calculate the gradient of the function with respect to the depth using the partial derivatives calculated in step 2;
6) Update the jet depth value using the gradient descent algorithm, which involves subtracting the gradient multiplied by a learning rate from the current value;
7) Repeated the process until the cost function reaches a minimum.

The cost function for the gradient descent optimiser is the modulus of the difference between $F_{z,jet}$ and $F_{z,jetpressure}$. A decision loop allows to determine if the cost function has reached a global minimum. The formulation of the cost function is:

$$J(h) = \left| F_{z,jet} - F_{z,jetpressure}(h) \right| \tag{8}$$

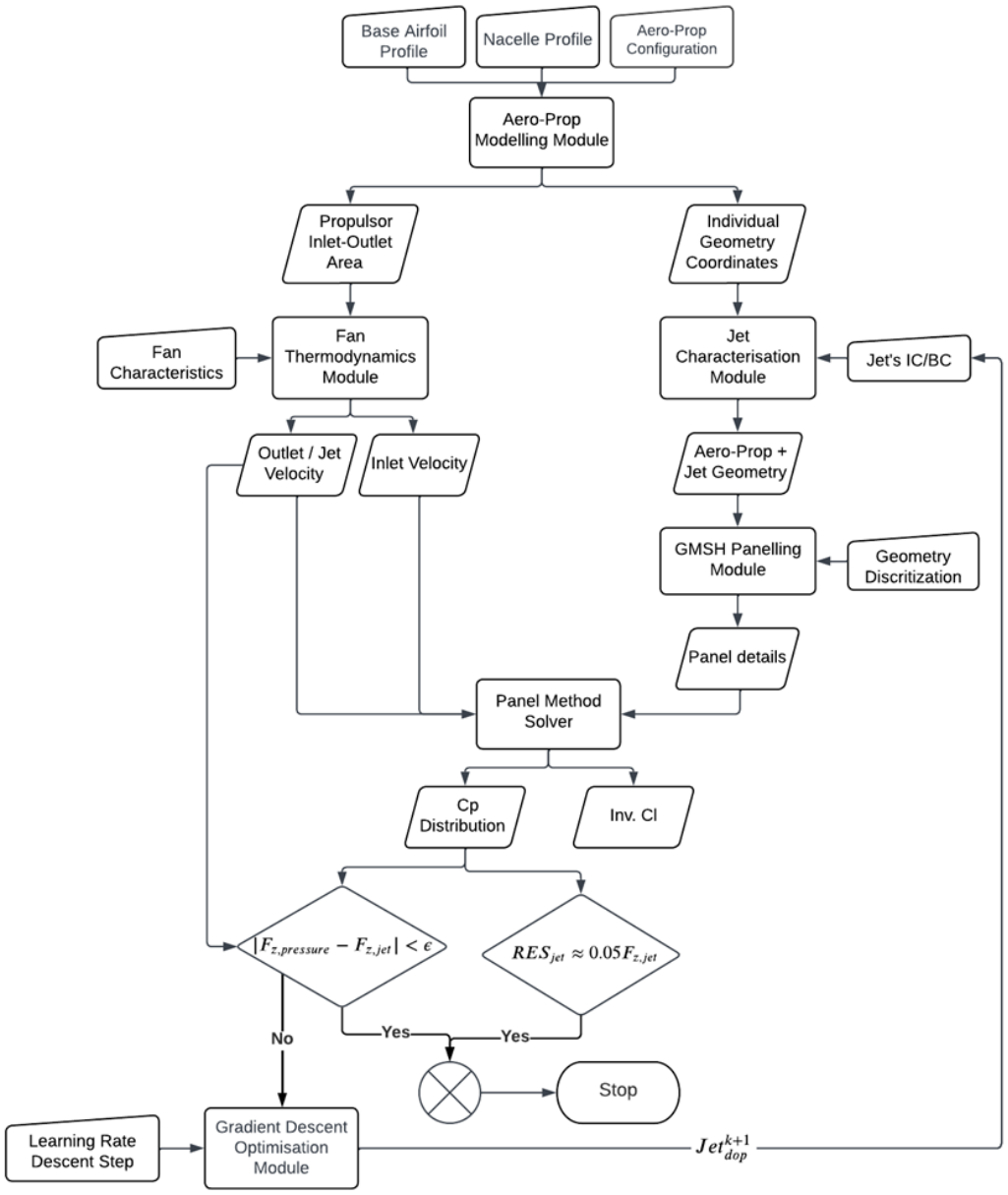

Fig. 7 The comprehensive routine of the presented panel-method tool for preliminary design of aero-propulsive configurations.

If the cost function has not reached a global minimum, this becomes the input for the gradient descent optimiser module. In order to determine the new jet depth, equation 9 can be used:

$$Jet_{dop}^{k+1} := Jet_{dop}^{k} - \alpha \cdot \left(\frac{\delta J}{\delta h}\right) \tag{9}$$

However, for the mathematical problem at hand it is challenging to determine the partial derivative of the cost function. Therefore, to calculate the partial derivative, a descent step (Δh) of appropriate size was chosen. Consequently, new vertical component of the integrated pressure force is determined. The difference in the vertical component of jet pressure force prior and latter to the step is calculated, which is then divided by the step size. This method becomes an efficient way to determine the partial derivative for the cost function if the derivatives cannot be determined analytically. This process is iterated until the cost function reaches a minimum, hence converging. Figure 6 presents the flow chart of the gradient descent algorithm module.

Combining the redeveloped routines for aero-propulsive modelling and the jet shape determination algorithm by with the previous tool for aero-propulsive architecture [9], the updated potential flow tool is established. The routine of the algorithm for the tool is illustrated in Figure 7.

V. Case Study and Preliminary Verification and Validation of the Tool

The above-described developments were accompanied with a preliminary verification and validation effort, discussed in this section. We begin with comparing the potential flow results for a clean airfoil with manufactured polar. Secondly, the potential flow tool results are compared to CFD analysis results for three chosen configurations out of numerous possibilities (some of which were represented in Figure 5).

A. Panel Method Comparison for Clean Airfoils

In order to provide some preliminary validation of the basic panel method implementation in the tool, clean airfoil cases were tested, whose results were then compared with C_l vs. α curves generated using *XFOIL* [15] for $NACA0010$, $S1210$, $MS313$ profiles. The tool is able to accurately predict the C_l vs α curve in the linear regime. (Fig.8)

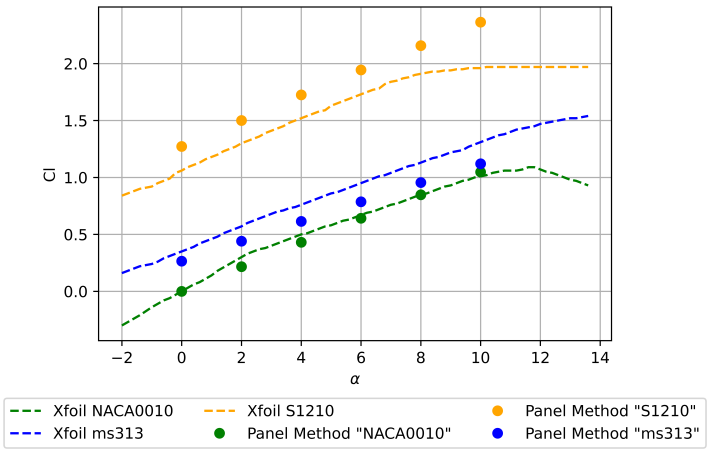

Fig. 8 Preliminary validation of the developed tool: comparison of the clean airfoil results against the *XFOIL* results for the same profile.

B. Aero-Propulsive Configuration Comparison with CFD Results

Since it is challenging to validate the tool against experiments, CFD analysis was utilised for further preliminary validation of the potential flow tool. Three different aero-propulsive configurations were chosen to represent the design space. Table 1 presents the geometrical details for the analysed configurations.

The presented configurations were analysed using CFD software *StarCCM+*. [16] The chosen CFD model was inviscid flow, chosen to make a most reasonable comparison of the results from the developed panel method tool and the

Table 1 Geometrical description of the configurations analysed using CFD.

Sr. No.	Base airfoil	Nacelle airfoil	c_{base}	$c_{nacelle}$	Nacelle relative angle	Nacelle LE offset	Vertical distance between foils
1	$ms313$	$naca0010$	2m	0.7m	7°	1.3m	0.4m
2	$ms313$	$naca0010$	2m	0.7m	7°	0.7m	0.4m
3	$ms313$	$naca0010$	2m	0.7m	−6°	0.7m	-0.4m

CFD. In order to automate the process of geometry generation, a geometry modelling tool was developed similar to the one employed in panel method tool. Furthermore, Python *GMSH* [17] API was used to generate geometries and flow domain compatible for CFD software. For each of the three mentioned configurations, a refined mesh was chosen which consisted of about 230k cells. These geometries were simulated at five angles of attack (0°, 2°, 4°, 6°, and 8°) for a free-stream velocity of 38 m/s. In order to optimise on the resources, and to have improved initialisation for the simulation, an iteration table was formed. This iteration table consisted of the information on V_x and V_y, which allowed to modify the angle of attacks in the simulation after the previous had converged. The boundary conditions imposed were wall for base and nacelle surfaces, velocity inlet for the propulsor inlet and outlet. To be noted, the velocity sign was negative for the inlet of the propulsor, and positive on the outlet. Velocities at the inlet and the outlet were calculated employing the *0D* thermodynamics module from the panel tool to be 128 m/s and 143 m/s, respectively.

Since the flow domain was rectangular, the domain inlet, the top and the bottom boundaries were defined as velocity inlet conditions, whereas the domain outlet was defined as pressure outlet boundary condition. Figure 9 illustrates the three analysed aero-prop configurations.

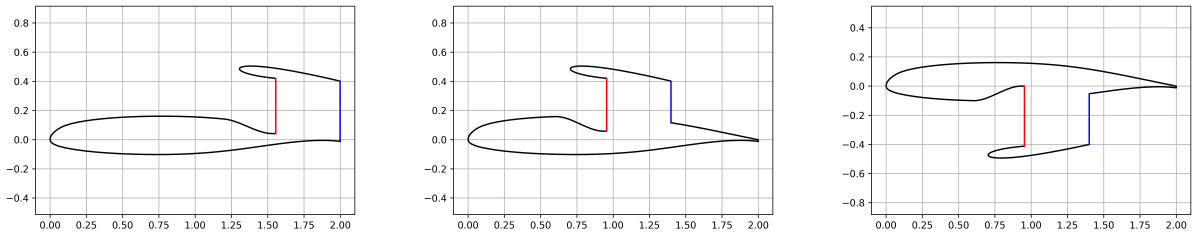

(a) Configuration 1 **(b) Configuration 2** **(c) Configuration 3**

Fig. 9 Aero-propulsive configurations drawn for analysis with CFD and with the panel tool.

These configurations were also analysed using the panel method tool and a comparison was made amongst the results of CFD and the panel tool. Cl vs α curves were compared for the two computation methods. Figure 10 illustrates the Cl vs α results of the three simulated configurations. It can be observed that when the nacelle is located on the suction side of the base airfoil, the lift produced is higher than when the case where the nacelle is located on the pressure side of the base airfoil. These trends are confirmed by both computation methods. It should also be considered that the pressure-side blown-wing configurations were analysed by Albers & Potter [10] which implicitly employed vectored thrust because of flap engagement. However, high-lift devices were not considered in the work presented in this paper, as the primary focus of exploring the aero-propulsive architectures was for exploring aircraft fuel consumption potential of such configurations, rather than for enabling short take-off and landing capabilities. Finally, despite the overall qualitative coherence of the respective configurations' individual trends, validity of the tool cannot be ascertained given the overall panel tool result quantitative deviation in comparison with the CFD results. Further analysis is mandated, as well as a comparison over a wider range of configurations.

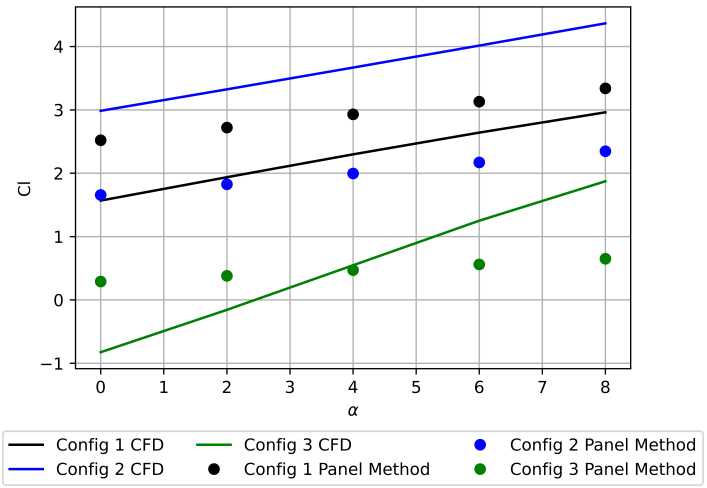

Fig. 10 C_l **vs** α **results obtained for the three configurations using CFD simulations and the panel tool.**

VI. Parametric Design Space Exploration Capability

Notwithstanding the difficulty in validating the results of the preliminary model, the tool's capability to explore the design space is evaluated by means of simple parametric studies with various features of the aero-propulsive assembly as free parameters.

Firstly, two sample parametric studies were done around the "Configuration 1" baseline case from Fig.5. The parameters that were varied are the propulsor inlet diameter and propulsive power in the first place (Fig.11), and in the nacelle angle and the configuration angle of attack on the other (Fig.12), and the response of the configurations lift coefficient C_l was observed. Both of the case groups were explored for a suction-surface- (left part of the figure) and

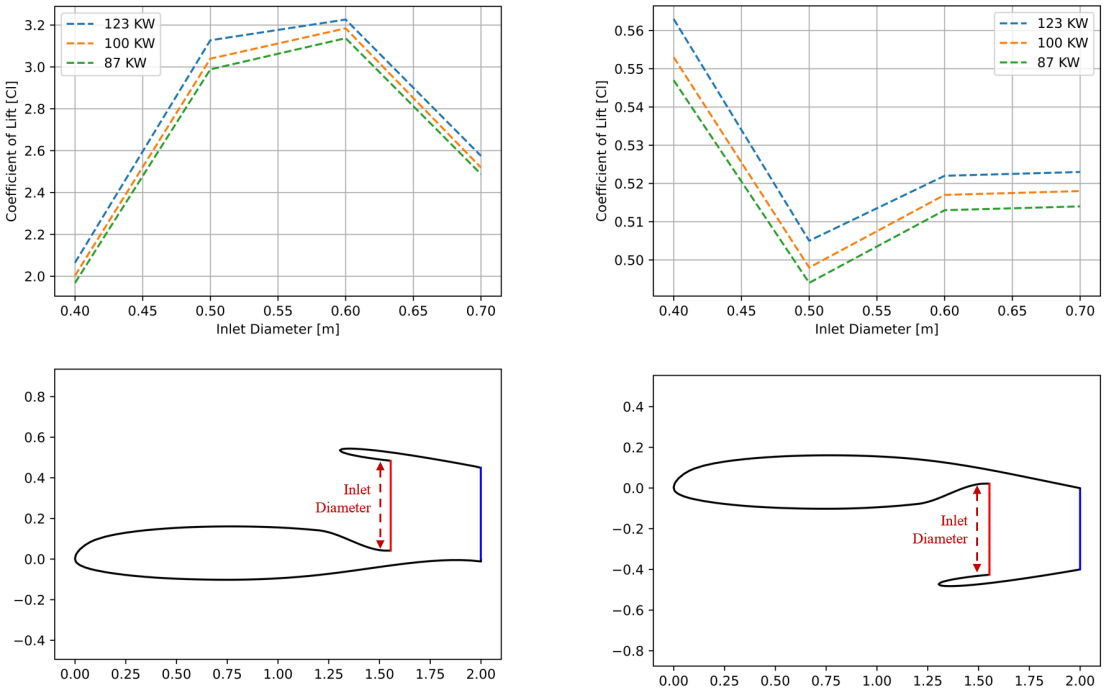

Fig. 11 C_l **vs Inlet diameter vs. fan power parametric study obtained using the panel tool.**

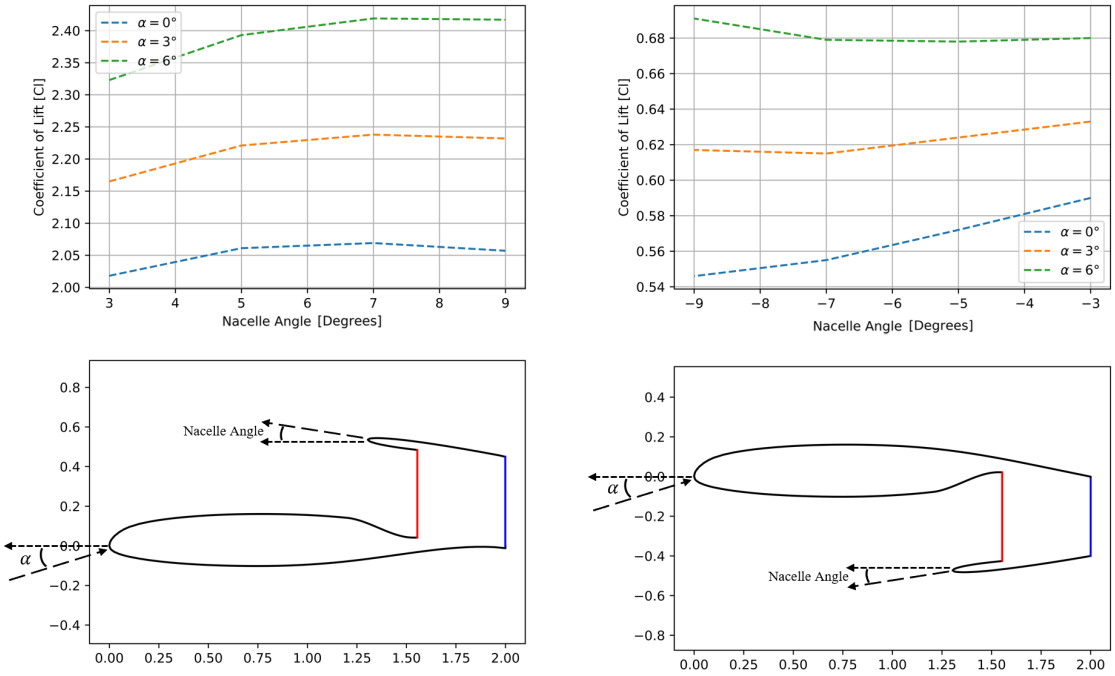

Fig. 12 C_l vs Nacelle angle vs. angle of attack parametric study obtained using the panel tool.

a pressure-surface-mounted propulsor configuration (right part of the figure). The overall qualitative C_l response to the respective parametrisations is satisfactory in that the resulting C_l curve variations do not exhibit any remarkable behaviour nor inconsistent tendencies (scattered results). In the propulsor diameter vs. power exploration (Fig.11), we can observe a tendency for the propulsive power increase to act beneficially on the lift curve overall, with lift loss at excessive propulsor diameters on the one hand, and on the other hand an unusual but not counter-intuitive behaviour with the pressure-side-propulsor configuration where the lift is reduced by increased flow velocity at the pressure side due to the presence of propulsor.

The nacelle angle vs. flow angle of attack study (Fig.12) the results similarly exhibit an intuitively correct tendency, in that the lift curve is beneficially influenced by the angle of attack variation, with penalties in the lift performance associated to excessive propulsor inlet "opening", albeit less penalising than the propulsor diameter increase seen in the parametric study above.

Furthermore, C_p distribution results are accessible with the tool. A sample presentation of such results is given for

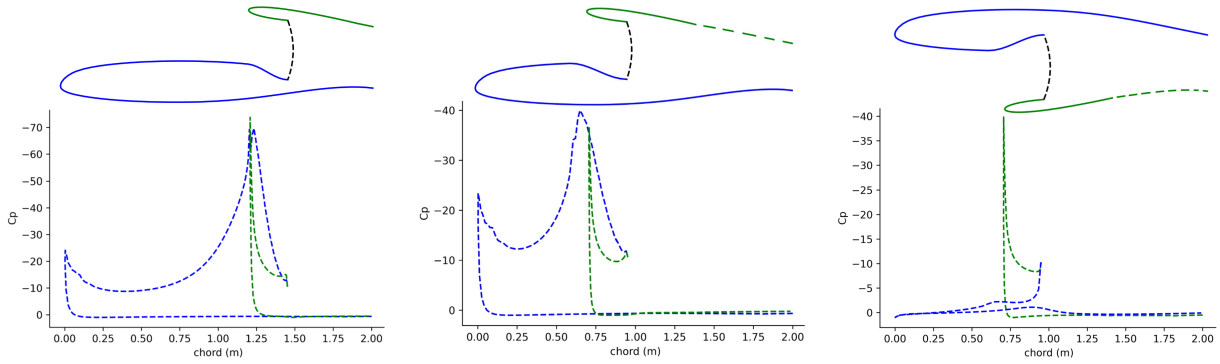

(a) Configuration 1 **(b) Configuration 2** **(c) Configuration 3**

Fig. 13 Calculated Cp distribution on the aero-propulsive assemblies at α = 2°.

the three architectures analogous to the ones previously simulated in CFD. (Fig.9) The resulting C_p distributions on the base and nacelle surface at an angle of attack of 2° (representative of conventional cruise angle of attack) are represented in Fig.13. The calculated trends indicate that a propulsor on the primary lifting surface suction side outperforms the case where propulsor is embedded on the pressure side of the base airfoil. However, the calculated C_l is higher for the case where the base airfoil is not in a blown configuration, contradictory to the results calculated with CFD. Moreover, the slopes of the C_l vs. α can be observed to be deviated when compared with the slopes obtained using CFD analysis.

The reader is reminded that these results serve only to qualitatively ascertain the feasibility of the tool when sweeping the parametric space of interest, whereas the quantitative validity of the results is yet to be made with further model tests and most of all - further refinements. Additionally, the authors want to bring light to the fact that the jet's boundary condition - specifically the jet exhaust angle (θ) - is a user input at the this stage of the development. While for the studied cases the jet exhaust angle (θ) is set constant to 0.1° (rather than 0°, to ease the convergence), it could be one of the reasons for deviation of results of panel method from the ones of CFD. Therefore, it would be essential to perform a multitude of CFD analysis spanning a broader design space to analyse the influence of the jet exhaust angle on various parameters such as - profile of the airfoil, angle of attack, propulsor power, nacelle relative angle, etc. This would allow finding the dependency of the jet exhaust angle of attack on the mentioned parameters and a possibility to automate the jet's boundary conditions management. While a parametric study is suggested by the authors for the jet bound. condition, for the future prospects one of population based optimisation techniques (Genetic Algorithm, Particle Swarm Optimisation) could be employed to determine the jet bound. conditions for the panel method tool.

VII. Conclusion: Ongoing and Future Work

This paper presented an in-house panel method tool that is capable of predicting the aerodynamic characteristics of two-dimensional aero-propulsive assemblies. The tool was developed/validated in two steps, which include application of the panel method to any two-dimensional configuration that allows independent manipulation of airframe geometric parameters and the propulsive power setting. The tool capabilities to resolve flow for clean airfoil is correct and coherent. On the other hand, it is not the case when modelling the aero-propulsive architectures, which was noted while comparing it with analogous Euler CFD calculations. The deviation seem to increase when moving the propulsor towards the leading edge, i.e. the blown wing configurations. It is reminded that the tool is not able to predict the influence on the lift coefficient by the part of the wing that is blown, which might be able to explain for the encountered problem in this part of the design space. Explorations are in progress to provide at least a rudimentary model to cover this zone and ascertain the newly-obtained results. The new jet shape determination module that employed gradient descent algorithm behaved better than the preceding code version, converging to a correct solution with handful of iterations. It should also be noted that the user input (jet exhaust angle θ) was found to be a crucial parameter affecting the accuracy of the results obtained from the tool. While full validation of the produced results yet has to take place, the current explorations indicate that the potential flow panel method tool for aero-propulsive architecture could provide a promising avenue for exploring and developing new aero-propulsive architectures for aircraft at computational costs compatible with conceptual design and preliminary sizing.

Ongoing works include integration of viscous coupling for rudimentary estimation of the boundary layer effects. For future prospects, it is suggested to perform a detailed parametric study using CFD analysis in order to identify the dependency of jet exhaust angle on various parameters such as profile of the airfoil, angle of attack, propulsor power, nacelle relative angle, etc. This, in turn, would enable the automation of jet boundary conditions and improve the accuracy of results obtained from the panel method tool. Furthermore, population-based optimization techniques like Genetic Algorithm and Particle Swarm Optimization could be employed to determine the jet boundary conditions.

Acknowledgments

The authors wish to express their gratitude to Vincent Maillet for his generous help with setting up the CFD calculations.

References

[1] Bijewitz, J., Seitz, A., Hornung, M., and eV, B., "A review of recent aircraft concepts employing synergistic propulsion-airframe integration," *30th Congress of the International Council of the Aeronautical Sciences, Daejeon, Korea*, 2016.

[2] Lee, D. S., Fahey, D. W., Skowron, A., Allen, M. R., Burkhardt, U., Chen, Q., Doherty, S. J., Freeman, S., Forster, P. M.,

Fuglestvedt, J., et al., "The contribution of global aviation to anthropogenic climate forcing for 2000 to 2018," *Atmospheric Environment*, Vol. 244, 2021, p. 117834.

[3] Kim, H. D., Felder, J. L., Tong, M., Armstrong, M., et al., "Revolutionary aeropropulsion concept for sustainable aviation: turboelectric distributed propulsion," Tech. rep., 2013.

[4] Plas, A., Crichton, D., Sargeant, M., Hynes, T., Greitzer, E., Hall, C., and Madani, V., "Performance of a boundary layer ingesting (BLI) propulsion system," *45th AIAA aerospace sciences meeting and exhibit*, 2007, p. 450.

[5] Uranga, A., Drela, M., Greitzer, E. M., Hall, D. K., Titchener, N. A., Lieu, M. K., Siu, N. M., Casses, C., Huang, A. C., Gatlin, G. M., et al., "Boundary layer ingestion benefit of the D8 transport aircraft," *AIAA journal*, Vol. 55, No. 11, 2017, pp. 3693–3708.

[6] Uranga, A., Drela, M., Hall, D. K., and Greitzer, E. M., "Analysis of the aerodynamic benefit from boundary layer ingestion for transport aircraft," *AIAA journal*, Vol. 56, No. 11, 2018, pp. 4271–4281.

[7] Wick, A. T., Hooker, J. R., and Zeune, C. H., "Integrated aerodynamic benefits of distributed propulsion," *53rd AIAA Aerospace Sciences Meeting*, 2015, p. 1500.

[8] Hendricks, E. S., "A Review of Boundary Layer Ingestion Modeling Approaches for use in Conceptual Design," Technical Memorandum NASA/TM-2018-219926, NASA Glenn, Cleveland,Ohio,US, 2018. URL `https://ntrs.nasa.gov/citations/20180005165`.

[9] Bommidala, H., Zambrano, E., Joksimović, A., Maillet, V., and Carbonneau, X., "Development of a Panel Method for Preliminary Design of Aero-Propulsive Systems," 2022.

[10] Albers, J. A., and Potter, M. C., *Potential flow solution for a STOL wing propulsion system*, Vol. 6394, National Aeronautics and Space Administration, 1971.

[11] Spence, D., "The lift coefficient of a thin, jet-flapped wing," *Proceedings of the Royal Society of London. Series A. Mathematical and Physical Sciences*, Vol. 238, No. 1212, 1956, pp. 46–68.

[12] Jois, H., and Ansell, P. J., "Analytical Framework for Design of Aero-Propulsive Geometries with Powered Wakes," *AIAA SCITECH 2023 Forum*, American Institute of Aeronautics and Astronautics, National Harbor, Maryland, USA, 2023. https://doi.org/10.2514/6.2023-1754, URL https://arc.aiaa.org/doi/10.2514/6.2023-1754.

[13] Katz, J., and Plotkin, A., *Low-speed aerodynamics*, Vol. 13, Cambridge university press, 2001.

[14] Farokhi, S., *Aircraft Propulsion*, 2nd ed., John Wiley & Sons, Inc., 2014.

[15] Drela, M., "XFOIL," , 2013. URL https://web.mit.edu/drela/Public/web/xfoil/.

[16] Simcenter, "STAR-CCM+," , (Date N/A). URL https://plm.sw.siemens.com/en-US/simcenter/fluids-thermal-simulation/star-ccm/.

[17] Geuzaine, C., and Remacle, J.-F., "Gmsh: A 3-D finite element mesh generator with built-in pre- and post-processing facilities," *International Journal for Numerical Methods in Engineering*, Vol. 79, No. 11, 2009, pp. 1309–1331. https://doi.org/10.1002/nme.2579, URL https://onlinelibrary.wiley.com/doi/abs/10.1002/nme.2579, _eprint: https://onlinelibrary.wiley.com/doi/pdf/10.1002/nme.2579.